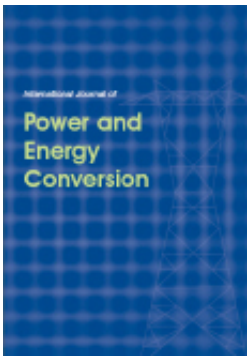

International Journal of Power and Energy Conversion

ISSN online: 1757-1162 - ISSN print: 1757-1154
https://www.inderscience.com/ijpec

Design of performance evaluation system for electrochemical energy storage power plants based on NSGA-II

Jiasheng Wu, Chao Dong, Bangjin Liu, Zheng Weng, Junyu Zhu

DOI: 10.1504/IJPEC.2025.10072494

Article History:

Received:	15 November 2023
Last revised:	01 February 2024
Accepted:	15 March 2024
Published online:	18 July 2025

Design of performance evaluation system for electrochemical energy storage power plants based on NSGA-II

Jiasheng Wu*, Chao Dong, Bangjin Liu, Zheng Weng and Junyu Zhu

CGS Power Generation (Guangdong) Energy Storage Technology Co., Ltd.,
Guangzhou, 510630, China
Email: jiasheng_wu666@outlook.com
Email: cnkjdongchao@126.com
Email: cnkjliubangjin@126.com
Email: wz1999@zju.edu.cn
Email: 15927653235@163.com
*Corresponding author

Abstract: Energy storage power stations can ensure the stability of wind and photovoltaic distribution networks, but the evaluation algorithms for measuring their reliability and economy are not comprehensive. The study proposes a performance evaluation system for electrochemical energy storage power plants based on an improved non-dominated sorting genetic algorithm. The experiment showed that compared with multi-objective particle algorithm and second-generation strength Pareto evolutionary algorithm, the research method had a better global optimisation level. The algorithm has been improved to increase its running and convergence speed by 3–5 times. An evaluation of the economic and reliability of the distribution network for a specific energy storage power station has been conducted. The annual return rates considering economy, reliability, and comprehensive coordinated investment were 13.05%, 9.05%, and 10.35%, respectively. This algorithm shows good reference value in terms of economic cost and technical reliability.

Keywords: NSGA-II; multi objective; performance evaluation; economy; reliability.

Reference to this paper should be made as follows: Wu, J., Dong, C., Liu, B., Weng, Z. and Zhu, J. (2025) 'Design of performance evaluation system for electrochemical energy storage power plants based on NSGA-II', *Int. J. Power and Energy Conversion*, Vol. 16, No. 5, pp.1–20.

Biographical notes: Jiasheng Wu graduated from South China University of Technology with a Master's in Fluid Machinery and Engineering in 2009, as a Senior Engineer. From April 2020 to July 2022, served as the Production Planning and Indicator Management Supervisor (Level 2) in the Production Technology Department of Peak shaving and Frequency Modulation Company. Technology Progress Award, in January 2018, he won the model worker of China Southern Power Grid, in June 2021, he won the Outstanding Communist Party Member, and in February 2021, he won the exemplary individual of Safe Production.

Chao Dong graduated from Wuhan University with a Master's in Power System and Automation in 2007, as a Senior Engineer. He served as a council member of the China Hydroelectric Engineering Society, a council member of the Guangdong Hydroelectric Engineering Society, and a member of the Intelligence and Intelligence Professional Committee of the China Hydroelectric Engineering Society. He is focusing on industries such as power monitoring systems, power equipment maintenance and operation, and the construction and operation of electrochemical energy storage power stations.

Bangjin Liu has a Bachelor's degree, graduated from Wuhan University in 2010 with a major in Energy Power Systems and Automation as a Senior Engineer. He has been engaged in research and engineering application of battery energy storage technology for over ten years, focusing on the application of integrated battery energy storage technology, research on battery operation safety technology, and management of battery energy storage power station engineering construction.

Zheng Weng graduated from Zhejiang University with a Bachelor's in Automation in 2021, focusing on the field of electrochemical energy storage construction. He works for China Southern Power Grid Peak Regulation and Frequency Modulation (Guangdong) Energy Storage Technology Co. Ltd., and has participated in the procurement, construction, commissioning, grid connection and acceptance of multiple new battery energy storage power stations in the past three years. He focuses on the cost composition and cost analysis of new energy storage projects. Meanwhile, we will supervise, review and summarise the compliance of the project in conjunction with national policies, laws and regulations.

Junyu Zhu (Han ethnicity), from Hezhou, Guangxi, graduated from the School of Artificial Intelligence and Automation at Huazhong University of Science and Technology in June 2022 with a Master's degree in Electronic Information. Since July 2022, he have been working as an Energy Storage Operation and Maintenance Engineer at Southern Power Grid Peak shaving and Frequency Regulation (Guangdong) Energy Storage Technology Co., Ltd., focusing on the operation and management of new energy storage power stations, the construction and operation of virtual power plants and energy storage control platforms, and the analysis of new energy storage big data.

1 Introduction

In the era of new energy development, the establishment and use of energy storage power plants (ESPPs) are gradually being valued, and the economic cost and reliability requirements for their distribution networks are also increasing. This multi-objective problem is commonly used in multi objective particle swarm optimisation algorithm (MOPSO), second generation strength pareto evolutionary algorithm (SPEA2), and non-dominated sorting genetic algorithm (NSGA-II) with elite strategy. This study selects NSGA-II, which has more advantages in convergence and global search ability. However, NSGA-II may encounter local optima when selecting an initial population with uncertainty and using simulated binary crossover operator (SBCO) to obtain offspring (Ryu et al., 2021). This study utilised a reverse solution for the initial population selection by implementing DNX instead of SBCO. This approach was taken to expand

the search range and increase the likelihood of obtaining the global optimal solution. Additionally, the elite selection strategy was improved, and population diversity was increased (Rezghi et al., 2020). A electrochemical ESPP performance evaluation system based on improved NSGA-II is proposed to reduce economic costs and improve efficiency, combining the economic and reliability evaluation of ESPP. The specific structure of the article is as follows. Firstly, it elaborates on the research significance and background of ESPP performance evaluation in the new resource era, as well as the research purpose of improving NSGA-II. Secondly, the specific principles and research process of NSGA-II optimisation are explained in detail, as well as the specific process and innovation points applied to ESPP performance evaluation. Then, the text fully elaborates on the experimental process design related to the algorithm evaluation and the quantitative statistics and analysis of the experimental results. Finally, the experimental conclusions, shortcomings in the research design, and directions for further in-depth research are described.

2 Related works

The establishment of electrochemical ESPP requires evaluation of its performance, and scholars have explored it from different perspectives. Bhogilla (2021) established and solved a two-dimensional numerical model to estimate the performance of the metal hydride energy storage system (MHESS) by studying the transient heat and hydrogen transfer characteristics of energy storage systems. It used the fully implicit finite volume method to handle the equations of the MHESS, achieving the calculation of thermal energy storage coefficient and providing a reference for performance evaluation. Cascetta et al. (2021) developed a comprehensive mathematical model for simulating daily behaviour and evaluating the annual performance of various TES technologies. Furthermore, a preliminary economic analysis was conducted and two alternative systems were proposed to replace the TES configuration. The use of a single tank heat storage system reduced investment costs and achieved good benefits for energy storage. Gonzalez et al. (2021) proposed an optimised sizing method for hybrid energy storage systems for renewable energy network integration. The battery aging caused by cycling was the main driving factor for optimal size, providing a reference for renewable resource storage. Alizadeh and his team (2020) conducted a comparative evaluation of the technical performance of two types of pumped storage hydropower stations (PSHSs): the doubly fed induction motor-based and the synchronous motor-based traditional PSHS. The safety, stability, and economy of the two PSHSs were demonstrated by using the discrete mode detailed model in MATLAB to simulate under different conditions. The results showed good performance in power grid auxiliary services. Based on the NSGA-II algorithm, Vukadinović et al. (2021) used software to dynamically simulate the combined operation of building heat and building structure. The optimisation results indicated that good results had been achieved in terms of building structure, heat storage capacity, and solar energy gain.

In solving the multi-objective problem of energy storage performance evaluation, scholars propose to combine the use of NSGA-II algorithm for research. Wu et al. (2023) proposed a grid-connected IES to study the multi-objective optimisation (MOO) problem of IES under the coupling mode of electrical, thermal, and cold energy. A MOO model was established and the MO-NSGA-II algorithm was proposed to solve the optimisation

model. It was indicated that MO-NSGA-II had superior self-regulation capacity, providing a reference for optimising comprehensive energy systems. Zhang et al. (2022a) proposed an Affine-Algorithm-based (AA-based) micro-grid Interval Optimisation (IO) method that considers uncertainty and BESS degradation. Introducing AA theory, a nonlinear BESS degradation cost model was proposed, and NSGA-II was used to perform the micro-grid IO framework. This IO method had good benefits in balancing simulation time and optimisation performance. Abdelshafy et al. (2020) proposed a new energy management strategy that uses NSGA-II to deal with the optimisation design of the system, while considering the minimum investment cost and minimum CO_2 emissions. The energy management strategy of this storage system was cost-effective from both economic and environmental perspectives. Zhang et al. (2022b) proposed a capacity allocation MOO method based on the improved NSGA-II algorithm for multi energy systems with multiple conflicting optimisation objectives for capacity allocation. The comparative analysis of the capacity configuration of off-grid and grid-connected multi energy systems showed that capacity configuration and operational strategies were effective and feasible for increasing the capacity of renewable energy and meeting the comprehensive performance requirements of multi energy complementary systems. Scholars such as Lasemi et al. (2021) used Monte Carlo simulation (MCS) method to model the uncertainty of wind. Combining NSGA-II to gain the Pareto optimal set, a new method for selecting the best possible solution was proposed based on the order performance entropy technique of TOPSIS method and the minimum-maximum regret criterion. This method was effective in solving the high uncertainty of wind farms in wind energy storage systems.

In summary, existing research focuses on analysing the specific characteristics of ESPP and proposing optimisation and improvement of its parameters. However, there is little research on improving the NSGA-II algorithm, and there is insufficient evaluation of the economy and performance of ESPP. This study aims to enhance the different algorithm stages of NSGA-II and utilise them for a comprehensive analysis of the performance and economic reliability of ESPP.

3 Improvement of NSGA-II and evaluation of ESPP performance

At present, the performance and improvement of ESPP are highly valued. This study aims to improve NSGA-II in various stages and apply it to the performance evaluation system of ESPP. A reliability and economic objective model is constructed to comprehensively evaluate the benefits of ESPP.

3.1 Optimisation design of NSGA-II by combining reverse learning mechanism and elite strategy

NSGA-II has disadvantages in application, such as high complexity, limitations in retaining the optimal individual, and the need for manual determination of parameter sharing. Professor Srinivas and Deb improved it to obtain NSGA-IIII, reducing the time complexity to O (mN^2) (Martínez et al., 2020). M is the quantity of objective functions (OFs) and N represents the population numbers. The principle of traditional fast non dominated genetic algorithm (GA) is Figure 1.

Figure 1 Principles of traditional fast non dominant gas (see online version for colours)

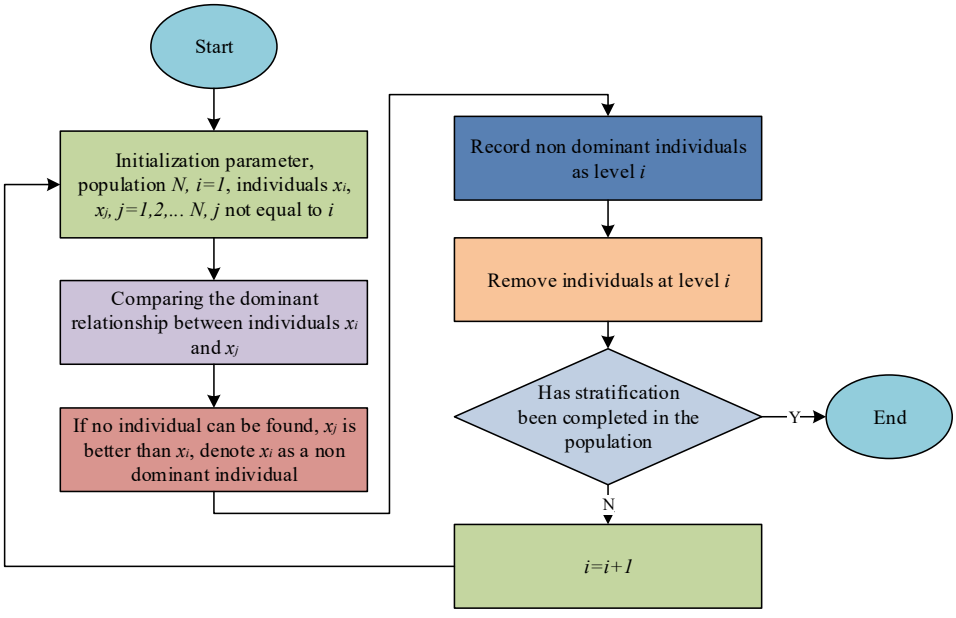

On this basis, the idea of crowding degree is came up with to address the problem of determining parameter sharing. Crowding degree is an expression that represents the density of individuals around an individual. Analysing non dominated individuals that have already been divided into levels can evaluate the density of other solutions. Judging population distribution through crowding has a good effect on understanding diversity (Alirahmi et al., 2021; Sadeghi et al., 2022). The calculation of congestion is segmented into several phases. Step 1 is to calculate the initial distance of individuals defining the same level, as shown in equation (1).

$$D(i) = 0 \tag{1}$$

Then, individuals at the same level are arranged in ascending order, and crowding analysis is performed on the centred individuals, as shown in equation (2).

$$D(i) = D(i) + \frac{f(i+1) - f(i-1)}{f_{\max} - f_{\min}} \tag{2}$$

In equation (2), $f(*)$ represents the OF value. f_{max} represents the largest individual arranged at the same level. f_{min} represents the smallest individual arranged at the same level. Then the ascending order is repeated and the crowding degree of each individual in the game is analysed until the crowding degree of all individuals is obtained. Figure 2 is an example of analysing the crowding degree of the OF (Cao et al., 2022).

Comparing the degree of crowding is beneficial for maintaining population diversity. Assuming f_1 and f_2 are two OFs in the state of optimisation to obtain the crowding degree of certain specific solutions in the population, an objective model is constructed to obtain the geometric mean distance of two points near specific points. Crowding degree refers to the circumference of the largest rectangle of other individuals near the point, and the

length of the box around the i^{th} solution represents its crowding degree (Zhang et al., 2021).

Figure 2 Schematic diagram of crowding degree between individuals analysed by OF

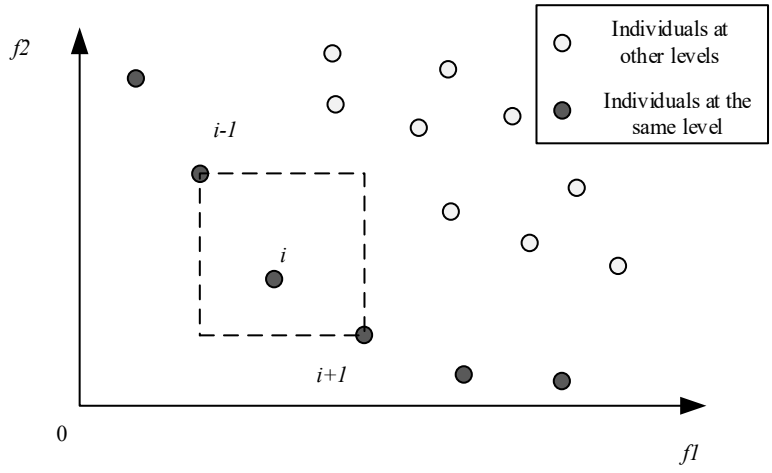

The elite selection strategy is aimed at improving the quality of the entire population and finding the optimal individual for protection. Two generations of population are considered as a single population, with a population size twice that of a single population. Then, the crowding degree of each individual is analysed and a fast non-dominated ranking is performed. Figure 3 shows the flowchart of the elite selection strategy. The new population $R(t)$ with a quantity of 2N is formed by mixing the offspring population $Q(t)$ with a quantity of N and the parent population $P(t)$. After completing the fast non dominated sorting, $P(t)$ obtains different levels of $Z(i)$. Then, the crowding degree of all individuals is analysed. The red dashed line represents the degree of crowding, and the portion above the dashed line represents individuals greater than the degree of crowding, which will be saved in $P(t + 1)$. The parts below the red dashed line indicate individuals who are less than the crowding level and do not have sufficient superiority, they will be eliminated. Until the individuals within $P(t + 1)$ equals N, the offspring population $Q(t + 1)$ is obtained through $P(t + 1)$.

Figure 3 Flowchart of elite selection strategy (see online version for colours)

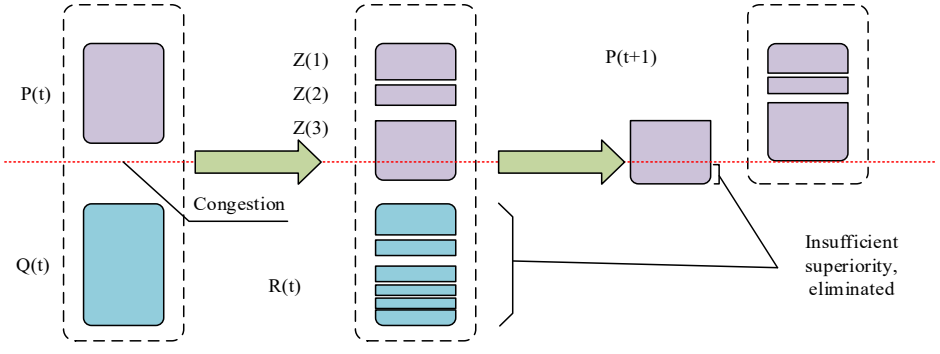

The tournament selection method of NSGA-II is a commonly used method, which allows some individuals to be selected multiple times during use, solving the problem of optimisation complexity caused by constraints. During the optimisation period of the population, the probability of selecting only a small number of individuals who meet the constraint conditions increases. These individuals replicate rapidly, which is not conducive to population diversity and leads to premature population convergence (Secchi et al., 2021).

The crossover process is the process of transmitting excellent genes from organisms to the next generation of individuals, promoting population evolution towards excellence. The SBCO is an improvement on binary single point crossover, as shown in equation (3).

$$\begin{cases} \begin{cases} x_{1,i}^{t+1} = 0.5\left[\left(1-\beta_i\right)x_{1,i}^{t} + \left(1-\beta_i\right)x_{2,i}^{t}\right] \\ x_{2,i}^{t+1} = 0.5\left[\left(1-\beta_i\right)x_{1,i}^{t} + \left(1-\beta_i\right)x_{2,i}^{t}\right] \end{cases} \\ \beta_i = \begin{cases} \left(2\mu_{c,i}\right)^{1/\eta_c+1}, \mu_i < 0.5 \\ \left[\dfrac{1}{2\left(1-\mu_{c,i}\right)}\right]^{1/\eta_c+1}, \mu_i > 0.5 \end{cases} \end{cases} \tag{3}$$

In equation (3), $x_{1,i}^{t+1}$ and $x_{2,i}^{t+1}$ respectively represent the true value encoding of the corresponding set variables for the two individuals of generation t. β_i represents random variables on all dimensions regenerated. μ_i means a uniformly distributed random number in the interval (0, 1). η represents a cross process parameter and is a non negative real number. The higher the η_c value, the closer the offspring are to the parent. Although SBCO can transmit superior parental genes to offspring through a crossover process, its global search performance is weak, which is not conducive to the development of population diversity (John et al., 2023).

The mutation process of GA is of great significance in increasing the local optimisation level, shortening the optimal solution time, and maintaining population diversity. The mutation process is equation (4).

$$\begin{cases} x_{1,i}^{t+1} = x_i^t + \alpha_i\left(x_{\max} - x_{\min}\right) \\ \alpha_i = \begin{cases} \left(2\mu_{m,i}\right)^{1/(\eta_m+1)} - 1, \mu_i < 0.5 \\ 1 - \left[\left(1-\mu_{m,i}\right)\right]^{1/\eta_m+1}, \mu_i > 0.5 \end{cases} \end{cases} \tag{4}$$

In equation (4), α_i represents a random variable. x_{max} and x_{min} represent the upper and lower limits of the x. $\eta_{m,i}$ is a random number uniformly distributed on the (0, 1). η_m represents the mutation parameter, similar to η_c.

NSGA-II has strong convergence and uniformity (C&U), but there are still some shortcomings. NSGA-II has uncertainty in the selection of the initial population, which may cause the population to fall into local optima, leading to premature convergence, and affecting the population's ability to obtain a global Pareto optimal solution set. This study has improved NSGA-II. Therefore, a reverse learning mechanism (RLM) is built to solve the matter of falling into local optima, as shown in equation (5).

$$X_{i,j}^{*} = a_i + b_j - X_{i,j}(i-1,2,...,N; j=1,2,...,D) \tag{5}$$

In equation (5), $X_{i,j}^{*}$ represents the component of the i^{th} chromosome distribution in the j^{th} dimensional space within the current population. $X_{i,j}^{*}$ represents the inverse solution represented by $X_{i,j}$. a_j and b_j represent the lowest and highest value of a gene in the j^{th} dimensional space of a chromosome. N represents the population size. D represents the spatial dimension of chromosomes. To perform reverse solving on all individuals, merging the initial forward population with the population obtained through reverse solving into a new population of $2N$. Calculating the chromosome fitness of all individuals and selecting N individuals with better fitness to form a new population, reducing the probability of local optima (Pascual et al., 2020).

The improvement of the selection process lies in increasing the diversity of the population. The elite selection strategy of NSGA-II is optimised by retaining the first level individuals that pass the screening, and then selecting individuals from other non-dominant levels, as shown in equation (6).

$$N_i = ceil\frac{2(M+1-i)N}{(M+2)(M-1)+2(M+1-i)}(2 \le i) \tag{6}$$

In equation (6), M represents the total number of population levels. i represents the current level of individual selection. $ceil(\cdot)$ represents obtaining an integer upwards. N_i represents the gross of selected individuals in layer i.

Improve the crossover process to address the limitations of search scope and the problem of population evolution towards the optimal population in specific environments. This study proposes the use of the normal distribution crossover (NDC) operator to increase the search range of the space and facilitate the acquisition of global optima. The improvement process is as follows: the parent generation is set to $x_{1,i}^{t+1}$ and $x_{2,i}^{t+1}$, the next generation is obtained through NDC as $x_{1,i}^{t}$ and $x_{2,i}^{t}$. Randomly to select a number as $r \in (0, 1]$. The crossover process of the i^{th} variable is equations (7) and (8).

For $r \le 0.5$, the calculation is equation (7).

$$\begin{cases} x_{1,i}^{t} = \dfrac{x_{1,t}^{t+1} + x_{2,t}^{t+1}}{2} + \dfrac{1.481\left(x_{1,t}^{t+1} - x_{2,t}^{t+1}\right)\left|N(0,1)\right|}{2} \\ x_{2,i}^{t} = \dfrac{x_{1,t}^{t+1} + x_{2,t}^{t+1}}{2} - \dfrac{1.481\left(x_{1,t}^{t+1} - x_{2,t}^{t+1}\right)\left|N(0,1)\right|}{2} \end{cases} \tag{7}$$

For $r > 0.5$, the calculation is equation (8).

$$\begin{cases} x_{1,i}^{t} = \dfrac{x_{1,t}^{t+1} + x_{2,t}^{t+1}}{2} - \dfrac{1.481\left(x_{1,t}^{t+1} - x_{2,t}^{t+1}\right)\left|N(0,1)\right|}{2} \\ x_{2,i}^{t} = \dfrac{x_{1,t}^{t+1} + x_{2,t}^{t+1}}{2} + \dfrac{1.481\left(x_{1,t}^{t+1} - x_{2,t}^{t+1}\right)\left|N(0,1)\right|}{2} \end{cases} \tag{8}$$

In equations (7) and (8), $|N(0, 1)|$ is a normally distributed random variable. In summary, the improvement process for NSGA-II is summarised in Figure 4. Firstly, relevant parameters are set and encoded, RLM is used to initialise the population, and some individuals are selected from each layer's non dominated solution set according to a certain proportion. To use crossover operators for crossover and mutation operations. The

parent and offspring populations are mixed to achieve elite retention strategy through rapid dominance sorting and crowding calculation, and ultimately to output the optimal.

Figure 4 Improvement process of NSGA-II (see online version for colours)

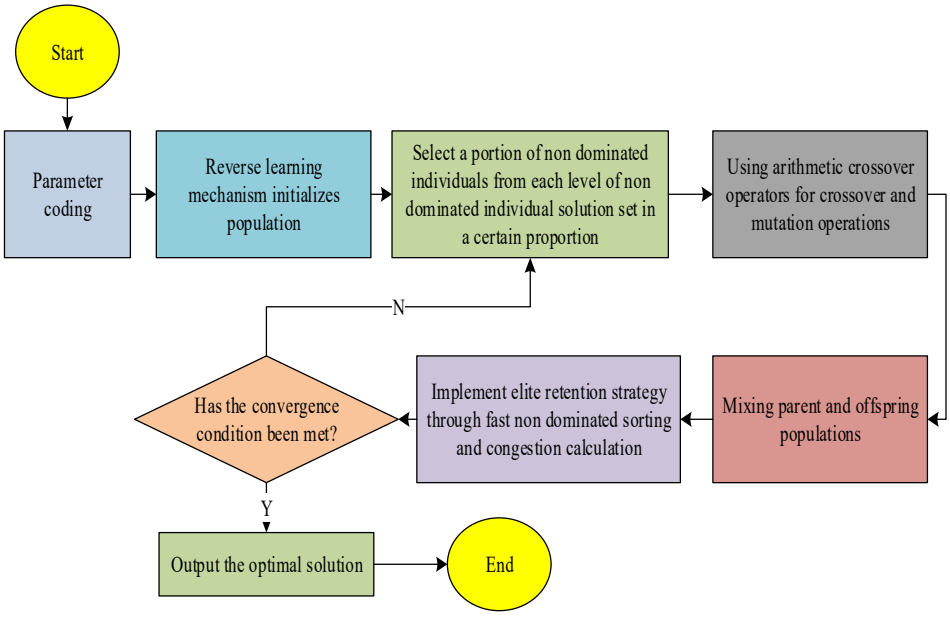

3.2 Performance evaluation of improved NSGA-II in electrochemical ESPP

In the era of new energy, there are high requirements for the planning and reliability of electrochemical ESPP distribution networks. However, if the planning is not reasonable, it will also increase the operating cost of ESPP. This study comprehensively evaluates the economic and reliability models of the distribution network for constructing ESPP. The calculation of economic benefits is equation (9).

$$\begin{cases} B_1 = \sum_{1}^{365}\sum_{i=1}^{24}\left(P_{id} - P_{ic}\right)R_i \\ B_2 = \lambda k_s P_h \\ B_3 = k_b \Delta P \\ C_1 = \left(k_e E_N + k_p P_N + k_f P_N\right)\dfrac{(1+e)^T}{T} \\ C_2 = k_r E_N \\ f_1 = B_1 + B_2 + B_3 - C_1 - C_2 \end{cases} \tag{9}$$

In equation (9), B_1 represents the electricity price gain obtained through the peak valley price difference. P_{id} and P_{ic} are the actual discharge and charging powers of ESPP at hour i. At any time, ESPP will only operate in one mode, namely charging or discharging

state. R_i represents the segmented electricity price in hour i. B_2 represents the capacity gain from reducing equipment capacity expansion. k_s represents the unit power price for equipment expansion. λ represents the asset depreciation rate. P_h represents the power of ESPP when the load reaches its peak. B_3 represents the policy subsidy benefits of the country. k_b represents the government subsidy benefit coefficient for successfully reducing unit peak load. ΔP represents the total load power transferred by ESPP annually. C_1 represents the annual equivalent initial investment cost. C_2 represents the annual maintenance cost (Saraswat and Saini, 2014).

$$\begin{cases} f_2 = R_{IEAR} \cdot E_{ENS} \cdot \lambda_s \left(1 - f\left(E_N < E_{ENS}\right)\right) + \left(\lambda_s - \lambda_s^{'}\right) E_\lambda \\ f\left(E_N < E_{ENS}\right) = h_{we} / 24 \\ E_{ENS} = T_s \left(1 - A_s\right) P_0 \\ \lambda_s^{'} = \lambda_s \lambda_b \left(r_s + r_b\right) \end{cases} \tag{10}$$

In equation (10), E_{ENS} represents the expectation that the important user's actual battery level is insufficient. λ_s and λ'_s represent the probability of power outages due to faults in the distribution network without or with ESPP construction. λ_b represents the failure rate of the energy storage battery (ESB). r_s and r_b represent the repair time for mains and ESB. E_N means the rated capacity of the ESB itself. E_λ is the expected value of losses caused by power supply interruption in production. T_s represents the actual annual production hours of the user. A_s represents the reliability of grid power supply. P_0 represents the lowest power during normal production for the user. h_{we} represents the number of hours when the battery level is less than E_{ENS}. $f(E_N < E_{ENS})$ represents the probability that the ESB cannot meet the normal production needs of important users. The objective model based on the economy and reliability of the distribution network established above is equation (11).

$$\max F = \left(f_1, f_2\right) \tag{11}$$

In practical applications of ESPP, ESB may face certain constraints. To avoid faults, it is important to maintain a *SOC* within a specific range and keep the battery's *SOC* updated, as demonstrated in equation (12). This is particularly important for batteries that do not experience linear overcharging or discharging.

$$\begin{cases} SOC_{\min} \le SOC \le SOC_{\max} \\ SOC(t+1) = \begin{cases} SOC(t) + \dfrac{P_{BESS}(t) \cdot \Delta t \cdot \eta}{E_{BESS}} \\ SOC(t) + \dfrac{P_{BESS}(t) \cdot \Delta t}{E_{BESS} \cdot \eta} \end{cases} \end{cases} \tag{12}$$

In equation (12), SOC_{max} and SOC_{min} represent the maximum and minimum (max–min) values of *SOC*. η represents the conversion efficiency of the ESB. Δt represents the charging and discharging (C&D) time of the ESB. For the power constraints of ESBs, it is necessary to ensure a cycle of normal use and energy conservation, as shown in equation (13).

$$\begin{cases} P_{BESS}^{\min} \le P_{BESS} \le P_{BESS}^{\max} \\ E_{\min} \le E \le E_{\max} \\ \sum_{i=1}^{24} \left(P_c(i) + P_d(i) \right) = 0 \end{cases} \tag{13}$$

In equation (13), $P_{BESS}^{\min}$ and $P_{BESS}^{\max}$ represent the min-max values of the C&D power of the ESB. E_{min} and E_{max} represent the min–max capacities of ESB. P_c and P_d represent the C&D power of the ESB.

Analysing multi-objective problems requires obtaining the optimal compromise solution. To do so, it is necessary to convert each objective function into comprehensive satisfaction for analysis. Then, the satisfaction of each optimal solution in each objective function can be analysed through a fuzzy membership function (Labbi et al., 2014). Fuzzy membership function is actually a function that maps the state variables of objective things to fuzzy sets. It can uniformly describe the state, characteristics, and other descriptive information of objective entities. This description is sometimes called membership function, which can be used to describe the attribute state of objective entities, making the descriptive information of objective entities more accurate and decision operable. The fuzzy membership function for solving the max–min problem of the OF is equation (14).

$$\begin{cases} h_{\min}(i) = \begin{cases} 1, f_i \le f_i^{\min} \\ \dfrac{f_i^{\max} - f_i}{f_i^{\max} - f_i^{\min}}, f_i^{\min} \le f_i \le f_i^{\max} \\ 0, f_i \ge f_i^{\max} \end{cases} \\ h_{\max}(i) = \begin{cases} 1, f_i \ge f_i^{\max} \\ \dfrac{f_i - f_i^{\min}}{f_i^{\max} - f_i^{\min}}, f_i^{\min} \le f_i \le f_i^{\max} \\ 0, f_i \ge f_i^{\min} \end{cases} \end{cases} \tag{14}$$

The corresponding curve represented by the membership function in equation (14) is Figure 5. The study employs a fuzzy logic controller's membership function to maximise the OF, which is represented by a fuzzy membership function. The OFs of the study are economic and reliability benefits, and therefore, the maximum value type membership function is selected.

Therefore, the satisfaction of all chromosome standardisation in the Pareto set is equation (15).

$$h = \frac{1}{N_{obj}} \sum_{i=1}^{N_{obj}} h_i \tag{15}$$

In equation (15), h represents the satisfaction degree of standardisation corresponding to chromosomes, and the higher the value of h, the higher the satisfaction degree. h_i represents the satisfaction of the i^{th} OF. $f_i^{\max}$ and $f_i^{\min}$ are the max–min values of the i^{th}

OF. f_i is the value of the i^{th} OF. N_{obj} represents the number of OFs. In summary, the improved NSGA-II electrochemical ESPP is used to build a distribution network economic and reliability comprehensive evaluation model, as shown in Figure 6.

Figure 5 The curve corresponding to the max-min values of the membership function (a) minimum value curve of fuzzy member function (b) curve maximum value of fuzzy membership function (see online version for colours)

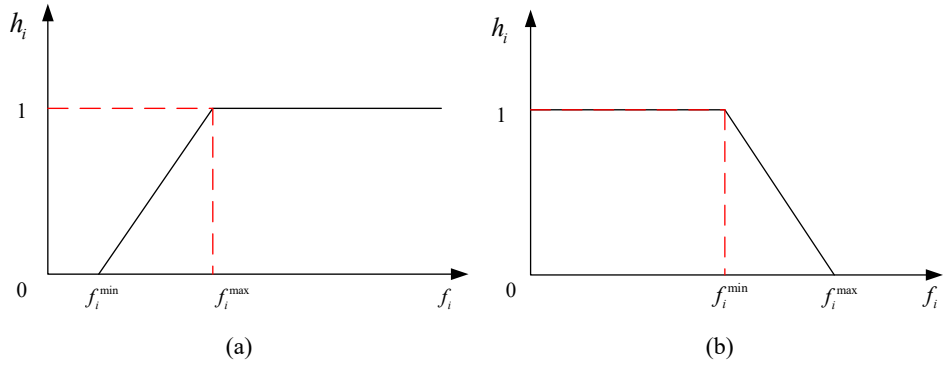

Figure 6 The implementation process of electrochemical ESPPS based on improved NSGA-II (see online version for colours)

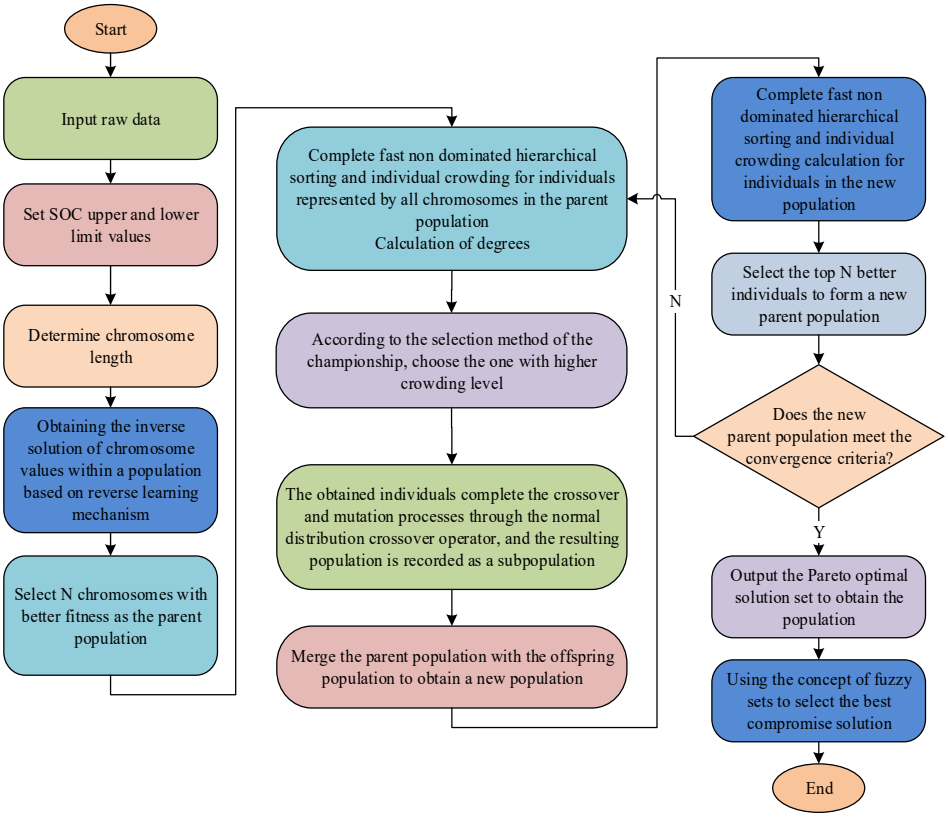

The selection of components mainly includes sensors, data acquisition cards, processors, and storage devices. Sensor selection is a high-precision sensor used to measure key parameters of electrochemical ESPPs, such as voltage, current, temperature, etc. A data acquisition card with high sampling rate, low noise, and low latency is selected to obtain data from the sensor. Processors with powerful computing and processing capabilities are selected, such as high-performance micro-controllers or industrial computers. Storage devices with large capacity and high reliability is selected to store data and algorithm execution results. The basic principle of selecting components is to select components that can accurately measure key parameters, quickly process data, and operate stably based on the performance evaluation requirements of electrochemical ESPPs. Meanwhile, considering the scalability and upgrade capability of the system, components with good compatibility and scalability are selected. When selecting components, it is necessary to consider parameters such as power consumption, size, weight, and cost. To improve the hardware implementation of NSGA-II, FPGA or GPU are chosen to achieve hardware acceleration of the improved NSGAII algorithm, which requires higher processing power. The integration and testing phase is the verification of the hardware implementation performance of components. The selected components are integrated into the performance evaluation system of the electrochemical ESPPs and comprehensive testing is conducted.

4 Experimental study on electrochemical ESPP performance evaluation system with improved NSGA-II

The experiment focuses on the designed electrochemical ESPP evaluation system based on NSGA-II, verifying the improvement effectiveness of the algorithm and its evaluation effect on ESPP. And it will be in contrast with other excellent MOO algorithms to verify the advantages of NSGA-II.

4.1 Experimental design for evaluation system validation

To validate the performance of the proposed algorithm, a stable and algorithmically supported cloud computing platform, Google Cloud Platform, was selected for online algorithm implementation in the experiment. This ensured that the experimental environment configuration met the operational requirements of the algorithm and had sufficient computing resources and storage capacity. An instance type with multiple vCPUs, high memory, and high-speed network connections was selected to ensure the speed and efficiency of model training. The operating system is Ubuntu 18.04 LTS. The experiment was analysed using the IEEE33 node model, as shown in Figure 7. The economic and reliability analysis of ESPP intervention in distribution networks containing lithium iron phosphate batteries under three different conditions of optimal OF economy, optimal reliability, and optimal coordination between economy and reliability. The relevant parameters are set, with an iteration count of 500, a population size of 220, a crossover probability of 0.92, and a mutation probability of 0.1. The upper and lower power limits of lithium iron phosphate batteries are 1.8 MW and 0.6 MW, respectively. The probability of C&D is 90%. The min–max state of charge are 0.1 and 0.9. Taking a certain city as an example, the peak period electricity price (PEP) is 1.1001 Yuan/kWh, the valley PEP is 0.3200 Yuan/kWh, and the average PEP is 0.6602 Yuan/kWh. The unit

power cost of other equipment in the distribution network is 50 W Yuan/MW, and the annual maintenance cost per unit capacity is 0.1 W Yuan/MW. The unit capacity price for delayed expansion is 100 W Yuan/MW. The government unit's peak valley transfer reward is 0.1 W Yuan/MW. The asset depreciation rate is set to 4%. The annual interest rate is 6.9 ‰.

The detailed information on the battery performance of a certain energy storage power station in the city studied in the experiment is shown in Table 1. Currently, the commonly used electrochemical energy storage devices in energy storage power stations include four categories: lithium-ion batteries, lead-acid batteries, all vanadium flow batteries, and sodium sulphur batteries. This study takes lithium batteries as an example, with a capacity of 100 Ah, a voltage of 48 V, a maximum charge and discharge current of 15 A, a power of 5 kW, a photovoltaic module specification of 5,000 W, a daily power generation of 16kWh, a conversion rate of 17.5%, and a warranty period of three years. Photovoltaic panels are the core part of photovoltaic power generation in energy storage power stations, with main parameters including power, voltage, and current, which are 540 W, 1,050 mm * 540 mm * 3 mm in size, and a weight of approximately 18.5 kilograms. The size of solar cells is 156 mm * 156 mm, and the working voltage is about 0.5V. After being packaged in series and parallel, solar cells become photovoltaic modules, with 60 or 72 cells per photovoltaic module. The photovoltaic panel has a short-circuit current of 6.06 A and is equipped with 32 batteries. Its working voltage and system voltage are both 18V, while its open circuit voltage is 21.6 V. The electricity generated by photovoltaic panels can generate 4.32 kWh, or approximately 4.32 kWh. According to the typical sunshine time of around 8 to 10 hours, 10 hours are taken, which is 5.4 kWh of electricity.

Figure 7 IEE33 node simulation example diagram (see online version for colours)

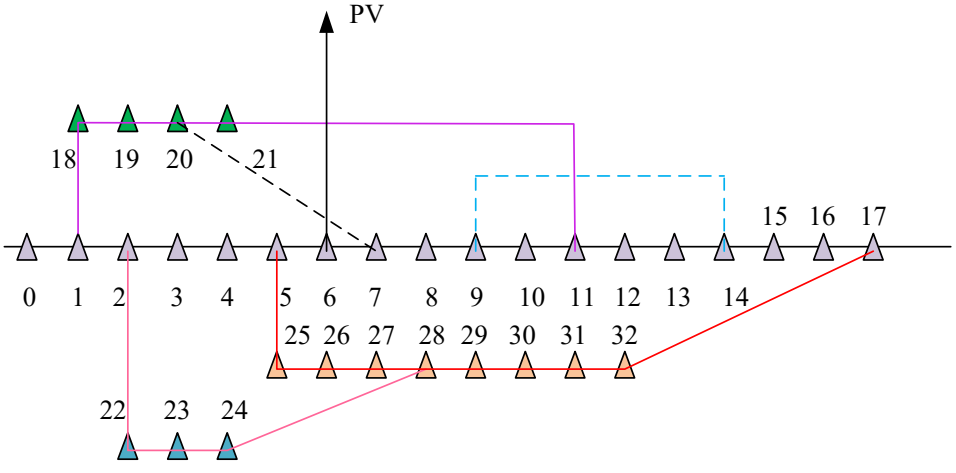

To conduct performance analysis on NSGA-II, comparisons were made with two MOO algorithms, MOPSO and SPEA2, as well as traditional GA. The experiment selected representative test functions of ZDT for performance testing. The algorithm's parameter settings include 200 iterations, 100 population. The binary operator crossover probability is 1, mutation probability is 1/n, and learning factors is 1.4801. The complexity of these four algorithms can be roughly arranged in the following order: MOPSO > NSGA-

II > GA > SPEA2. The adjustment parameters for MOPSO are 200 particles, 0.3 inertia factor, 0.28 individual learning factor, and 0.26 group learning factor. GA adjusts the parameters to population size of 200, crossover probability of 0.24, and mutation probability of 0.29. NSGA-II adjusts the parameters to polynomial mutation operator, with upper and lower bounds of 0.8 and 0.1 for decision variables, mutation distribution index of 0.4, and mutation rate of 0.3. The SPEA2 adjustment parameter is a population size of 200, and the fitness allocation calculation formula is $F(i) = R(i) + D(i)$. Among this, $R(i)$ represents the sum of the number of individuals dominated by all dominant individuals j, and $D(i)$ is the inverse function of the distance from individual i to its k^{th} neighbouring individual. The effectiveness of NSGA-II before and after improvement was analysed, setting algorithm parameters similar to algorithm comparison experiments. The operators SBCO and NDC were selected, the NSGA-II algorithm was simulated 25 times on the test function before and after improvement, and the corresponding GD index, SP index, and average algorithm running time were statistically calculated. Conducting pre data processing experiments reveals that the root cause of errors is mainly due to approximation or rounding errors in the algorithm, which may lead to inaccurate calculation methods.

Table 1 Detailed information on battery performance of an energy storage power station in the City

Battery equipment	*Energy density*	*Power density*	*Energy conversion efficiency*	*Power level*
Lithium iron phosphate battery	120–150 Wh/kg	1,500–2,000 W/kg	85–95%	> 0–100 MW
Lithium titanate battery	60–80 Wh/kg	3,000 W/kg	> 95%	0–32 MW
Nickel cobalt manganese lithium battery	170–220 Wh/kg	3,000 W/kg	> 95%	0–32 MW
Traditional lead-acid batteries	25–50 Wh/kg	< 150 W/kg	70–85%	0–20 MW
Lead carbon battery	25–50 Wh/kg	150–500 W/kg	70–85%	0–20 MW
All vanadium flow battery	7–15 Wh/kg	10–40 W/kg	75–85%	0.03–10 MW
Zinc bromine flow battery	65 Wh/kg	200 W/kg	75–80%	0.05–2 MW
Sodium sulphur battery	88 Wh/kg	16.6 W/kg	90%	0–50 MW

4.2 Statistical analysis of experimental results

The experiment compared the economic and reliability benefits of NSGA-II in the construction of ESPP for distribution networks under three different conditions before and after improvement, as shown in Table 2. By comparing the benefits of three scenarios before and after improving NSGA-II, building ESPP can improve the economic and reliability benefits of the distribution network, but the two will affect each other. The total benefits obtained when considering the optimal coordination of economy and reliability are not as good as those obtained solely under a single scenario. In the same

situation, the improved algorithm yields higher returns, indicating that the improved NSGA-II has better global search capabilities. After improvement, the annual return on investment for scenario 1 is 13.05%, scenario 2 is 9.05%, and scenario 3 is 10.35%. There was a small decrease in power before and after the algorithm was improved, which resulted from the algorithm's more precise optimisation, leading to reduced power consumption but greater overall benefits. The annual return analysis shows that all three scenarios have investment prospects and are higher than the return on investment under the same conditions before improvement. At present, the investment and construction of ESPP is the most common in situation 3.

Table 2 NSGA-II before and after improvement in three different situations for economic and reliability benefits of distribution networks

Situation	*Improved NSGA-II optimal value*				*NSGA-II optimal value before improvement*			
	Energy storage power station power/MW	*ESPP capacity/ MWh*	*f1/ 10,000 Yuan*	*f2/ 10,000 Yuan*	*Energy storage power station power/MW*	*ESPP capacity/ MWh*	*F1/10,000 Yuan*	*f2/ 10,000 Yuan*
1	1.121	3.854	472.51	20.15	1.255	3.948	456.84	16.57
2	1.482	5.947	427.35	67.81	1.658	6.184	412.35	61.75
3	1.305	4.956	488.53	35.61	1.385	5.987	432.8	30.55

Figure 8 (a) NSGA-II Pareto optimisation curve before and after improvement (a) NSGA-II Pareto optimisation curve before improvement (b) improve NSGA-II Pareto optimisation curve (see online version for colours)

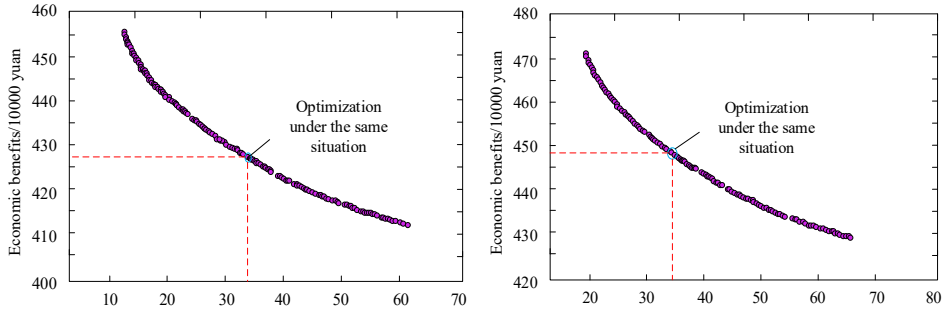

(a) (b)

To visually analyse the advantages of NSGA-II before and after improvement, a Pareto optimisation curve was drawn as shown in Figure 8. The balance between economic benefits and reliability benefits obtained from the compromise solution is indicated by the arrow. Figures 8(a) and 8(b) shows the differences in system optimisation before and after the algorithm improvement. In the same situation, the results obtained by using improved NSGA-II are greater than those without improved NSGA-II. The optimisation results using improved NSGA-II in the early stage showed a significantly faster decrease rate, indicating that the improved NSGA-II improved its global optimisation level in the

early stage. The resulting economic and reliability benefits are greater, indicating that the improved NSGA-II has a stronger level of optimisation.

Table 3 shows the GD and SP indicators of NSGA-II before and after typical test function improvement, and compares them with the results of the GA. The NSGA-II values of GD and SP indicators for ZDT1, ZDT2, ZDT3, and ZDT6 are the lowest. The smaller the indicator value, the closer the solution obtained by the algorithm is to the true boundary. The GD and SP values of NSGA-II are smaller than those of other algorithms, and compared to GA, it indicates that the C&U of NSGA-II is better than that of MOPSO and SPEA2.

Table 3 GD and SP index of ZDT1, ZDT2, ZDT3, and ZDT6 before and after NSGA-II improvement, and comparison with GA

Algorithm	*GD indicator*				*SP indicator*			
	ZDT1	*ZDT2*	*ZDT3*	*ZDT6*	*ZDT1*	*ZDT2*	*ZDT3*	*ZDT6*
MOPSO	0.1085	0.0645	0.1284	0.1094	0.0836	0.0849	0.1058	0.0847
SPEA2	0.6821	0.0268	0.0297	0.0498	0.0719	0.0758	0.0987	0.0716
NSGA-II	0.0479	0.02158	0.0271	0.0285	0.0615	0.0614	0.0821	0.0648
GA	0.1523	0.0924	0.0415	0.0519	0.0741	0.0754	0.0998	0.0921

Figure 9 Results of GD and SP indicators before and after NSGA-II improvement (see online version for colours)

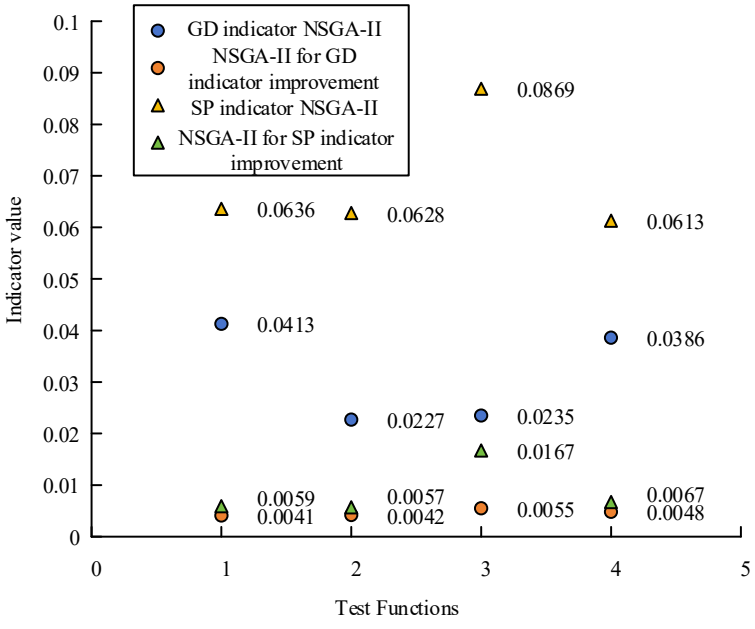

Figure 9 shows the results of GD and SP indicators before and after NSGA-II improvement. In representative ZDT test functions, the lower the function value, the better the C&U of the algorithm. The improved NSGA-II shows significant advantages, with GD and SP indicators close to 0. This algorithm has stronger global search ability

and running speed, and the obtained solutions have better convergence and more uniform spatial distribution.

From the comparison between the Pareto optimal solution and the real solution in Figure 10, in ZDT2, the improved NSGA-II has fewer breakpoints, and the obtained solution is closer to the real Pareto frontier than the NSGA-II solution, with better convergence. The improved NSGA-II has significantly more solutions for a certain two segments, and its global search ability is better than NSGA-II. Therefore, the improved NSGA-II has better performance.

Figure 10 Comparison between the Pareto value test results of NSGA-II in ZDT2 before and after improvement and the actual value (a) test results of NSGA-II in ZDT2 (b) improve NSGA-II results in ZDT2 (see online version for colours)

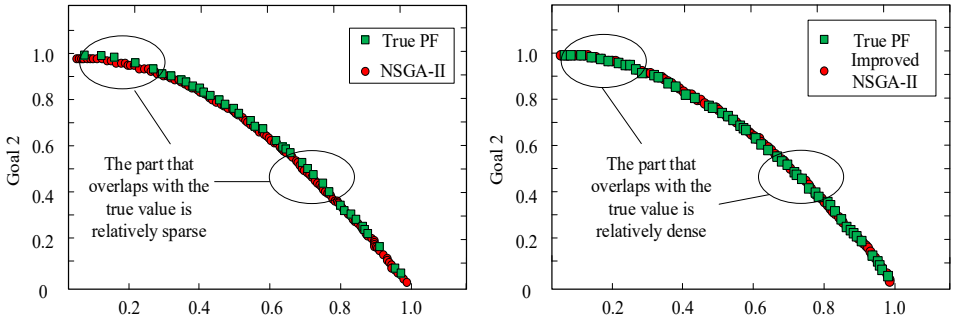

From the average running time of the two algorithms in Table 4, the improved NSGA-II runs more than twice as fast as NSGA-II, with the highest speed approaching five times.

Table 4 Average running time before and after algorithm improvement

/	*NSGA-II*	*Improved NSGA-II*	*GA*
ZDT1	4.7625	2.6954	5.3521
ZDT2	7.4012	2.7619	5.8124
ZDT3	12.8451	2.9984	8.1574
ZDT6	15.2715	3.2251	9.2558

5 Conclusions

The performance analysis and economic and reliability evaluation of ESPP distribution network provided reference for new energy storage. This study was based on multi-objective algorithm for NSGA-II optimisation, improving the initial population selection. The selection of elite strategies and the cross process were improved using NDC. An analysis was conducted on the economy and reliability of the distribution network of ESPP, and a corresponding model was established. A reliability model was established using sequential Monte Carlo method, and an ESPP performance analysis system grounded on improved NSGA-II was established. This study conducted simulation experiment analysis using MATLAB. The data showed that when comparing

the running time of the NSGA-II in the pre- and post-improvement, the speed of the improved NSGA-II algorithm was much faster than before, approaching 5 times faster and at least 2 times faster. The convergence speed and efficiency of the algorithm had been effectively improved, reducing time costs. The improved NSGA-II showed significant advantages, with GD and SP indicators close to 0. This indicated that the improved NSGA-II algorithm had stronger global search ability and running speed, and the obtained solutions had better convergence and more uniform spatial distribution. In the comprehensive evaluation of the economic reliability of ESPP, the improved annual return on investment for scenario 1 was 13.05%, scenario 2 was 9.05%, and scenario 3 was 10.35%. The topology structure can reflect the specific structure, faults, and risks of the current ESPPs. In a topology, multiple paths can be formed between nodes. When one path fails, other paths can continue to maintain the normal operation of the network and have high reliability. The topology structure has strong scalability and can be flexibly expanded according to needs, making it easy to add or reduce nodes without affecting the stability of the entire network. When a network failure occurs, the connection relationships between nodes in the topology structure are clear and easy to locate. However, when discussing ESPP in this study, only simulation analysis was used for validation, and the results were too ideal. The practical application of ESB in ESPP is limited by their inconsistency, which in turn limits their use in distribution networks. Therefore, simple access methods cannot be used to analyse them. The characteristics of ESB need to be comprehensively considered.

References

Abdelshafy, A.M., Jurasz, J. and Hassan, H. (2020) 'Optimized energy management strategy for grid connected double storage (pumped storage-battery) system powered by renewable energy resources', *Energy*, 1 February, Vol. 192, No. 1, pp.116615.1–116615.16.

Alirahmi, S.M., Razmi, A.R. and Arabkoohsar, A. (2021) 'Comprehensive assessment and multi-objective optimization of a green concept based on a combination of hydrogen and compressed air energy storage (CAES) systems', *Renewable and Sustainable Energy Reviews*, May, Vol. 142, No. 3, pp.110850.1–110850.20.

Alizadeh, B.M., Yang, W.J. and Ahmadian, A. (2020) 'DFIM versus synchronous machine for variable speed pumped storage hydropower plants: a comparative evaluation of technical performance', *Renewable Energy*, October, Vol. 159, No. 86, pp.72–86.

Bhogilla, S.S. (2021) 'Numerical simulation of metal hydride based thermal energy storage system for concentrating solar power plants', *Renewable Energy*, Vol. 172, No. 3, pp.1013–1020.

Cao, Y., Dhahad, H.A., Alsharif, S., El-Shorbagy, M.A., Sharma, K., Anqi, A.E., Rashidi, S., Shamseldin, M.A. and Shafay, A.S. (2022) 'Predication of the sensitivity of a novel daily triple-periodic solar-based electricity/hydrogen cogeneration system with storage units: dual parametric analysis and NSGA-II optimization', *Renewable Energy*, June, Vol. 192, No. 1, pp.340–360.

Cascetta, M., Petrollese, M., Oyekale, J. and Cau, G. (2021) 'Thermocline vs. two-tank direct thermal storage system for concentrating solar power plants: a comparative techno♂conomic assessment', *International Journal of Energy Research*, Vol. 45, No. 12, pp.17721–17737.

Gonzalez-Gonzalez, J.M., Martin, S., Lopez-Perez, P. and Aguado, J.A. (2020) 'Hybrid battery-ultracapacitor storage system sizing for renewable energy network integration', *IET Renewable Power Generation*, Vol. 14, No. 13, pp.2367–2375.

John, Y.M., Sanusi, A., Yusuf, I. and Modibbo, U.M. (2023) 'Reliability analysis of multi-hardware–software system with failure interaction', *Journal of Computational and Cognitive Engineering*, Vol. 2, No. 1, pp.38–46.

Labbi, Y. and Benattous, D. (2014) 'A genetic algorithm to solve the thermal unit commitment problem',I*nternational Journal of Power and Energy Conversion*, Vol. 5, No. 4, pp.344–360.

Lasemi, M.A., Arabkoohsar, A. and Hajizadeh, A. (2021) 'Stochastic multi-objective scheduling of a wind farm integrated with high-temperature heat and power storage in energy market', *International Journal of Electrical Power and Energy Systems*, Vol. 132, No. 6, pp.107194.1–107194.15.

Martínez, S., Pérez, E. and Eguía, P. (2020) 'Model calibration and exergoeconomic optimization with NSGA-II applied to a residential cogeneration', *Applied Thermal Engineering*, Vol. 169, No. 14, ppp.114916.1–114916.14.

Pascual, S., Lisbona, P., Bailera, M. and Romeo, L.M. (2020) 'Design and operational performance maps of calcium looping thermochemical energy storage for concentrating solar power plants', *Energy*, 1 April, Vol. 220, No. 4, pp.119715.1–119715.11.

Rezghi, A., Riasi, A. and Tazraei, P. (2020) 'Multi-objective optimization of hydraulic transient condition in a pump-turbine hydropower considering the wicket-gates closing law and the surge tank position', *Renewable Energy*, April, Vol. 148, No. 4, pp.478–491.

Ryu, K., Lee, T., Baek, D., Park, J. and Kim, N. (2021) 'A study on accumulator analysis for the valve performance evaluation system of nuclear power plants', *Kerntechnik*, Vol. 86, No. 1, pp.39–44.

Sadeghi, D., Ahmadi, S.E., Amiri, N., Marzband, M., Abusorrah, A. and Rawa, M. (2022) 'Designing, optimizing and comparing distributed generation technologies as a substitute system for reducing life cycle costs, CO_2 emissions, and power losses in residential buildings', *Energy*, 15 August, Vol. 253, No. 8, pp.123947.1–123947.27.

Saraswat, A. and Saini, A. (2014) 'Principal component analysis-based real coded genetic algorithm for optimal reactive power dispatch', *International Journal of Power and Energy Conversion*, Vol. 5, No. 2, pp.135–154.

Secchi, M., Barchi, G., Macii, D., Moser, D. and Petri, D. (2021) 'Multi-objective battery sizing optimisation for renewable energy communities with distribution-level constraints: a prosumer-driven perspective', *Applied Energy*, Vol. 297, No. 5, pp.17171.1–117171.13.

Vukadinović, A., Radosavljević, J., Đorđević, A., Protić, M. and Petrović, N. (2021) 'Multi-objective optimization of energy performance for a detached residential building with a sunspace using the NSGA-II genetic algorithm', *Solar Energy*, Vol. 224, No. 8, pp.1426–1444.

Wu, X., Liao, B., Su, Y. and Li, S. (2023) 'Multi-objective and multi-algorithm operation optimization of integrated energy system considering ground source energy and solar energy', *International Journal of Electrical Power and Energy Systems*, January, Vol. 144, No. 1, pp.108529.1–108529.16.

Zhang, G., Wang, W., Du, J. and Sheng, H. (2021) 'Multiobjective economic optimal dispatch for the island isolated microgrid under uncertainty based on interval optimization', *Mathematical Problems in Engineering*, Vol. 2021, No. Pt.42, pp.983104.1–9983104.14.

Zhang, X., Son, Y., Cheong, T. and Choi, S. (2022) 'Affine-arithmetic-based microgrid interval optimization considering uncertainty and battery energy storage system degradation', *Energy*, 1 March, Vol. 242, No. 5, pp.123015.1–123015.16.

Zhang, Y., Sun, H., Tan, J., Li, Z., Hou, W. and Guo, Y. (2022) 'Capacity configuration optimization of multi-energy system integrating wind turbine/photovoltaic/hydrogen/battery', *Energy*, 1 August, Vol. 252, No. 8, pp.124046.1–124046.18.